http://dx.doi.org/10.5012/bkcs.2013.34.11.3265

Characteristics of the Multi-Hydrogen Bonded Systems: DFT Description on the Solvated Electrons

Jun Xu

Department of Quality Detection and Management, Henan University of Animal Husbandry and Economy, Zhengzhou 450011, China. E-mail: xj_chem@163.com
Received March 12, 2013, Accepted August 10, 2013

The multi-hydrogen bonded systems with the solvated electrons are investigated at the B3LYP/6-311++G** basis set level. The symmetrical linear geometrical characteristic is common for the dimer systems, while for the tetramer system, the tetrahedron configuration is generated. The NBO charge analyses demonstrate that the multi-hydrogen-multi-electron (*mH-ne*) coupling exist in these anion systems, as is supported by the electrostatic potential and the molecular orbital analyses. The positive chemical shift value of the central hydrogen (H_c) and the negative chemical shift value of the terminal hydrogen (H_t) indicate that the H_c is electronegative while the H_t is electropositive, respectively. Strong coupling between two central hydrogen atoms is demonstrated by the large spin-spin coupling constants. The solvated electron donates significant contributions for the stability of these systems.

Key Words : Multi-hydrogen bond, NBO analysis, Electrostatic potential, NMR, DFT

Introduction

The hydrogen, which is abundant and exists in various configurations, can generate the covalent bond with electronegative atoms or make the metal hydride with the electropositive metal atoms. The hydrogen plays vital roles in the fields of biology, chemistry, and materials. The typical hydrogen bond has been extended with the observation of dihydrogen bond,[1-7] which consists of $H^{\delta+}\cdots H^{\delta-}$ and $H^{\delta+}\cdots e\cdots H^{\delta+}$ two forms. The significance of the solvated electron in such systems has been emphasized specifically.[8,9] A comprehensive *ab initio* study was performed on the wet electron – an electron interacting with a small cluster of water molecules – in the water hexamer system, providing the nature of a wet electron.[10] The monoelectron dihydrogen bond H···e···H in the anionic $(FH)_n\cdots e\cdots(HF)_n$ clusters has been described.[11] The application of solvated electron in the enhancement of hydrogen storage ability of metal hydride has been addressed.[12] Along with the development of the science, the knowledge about the nature of hydrogen is deepen and comprehensive gradually. H_3^+ is taken as the cornerstone of interstellar chemistry because it initiates the reactions responsible for the production of many larger molecules observed in the interstellar medium.[13,14] The time evolution of electron density descriptors in H_3^+ and LiF is defined by the quantum theory of atoms in molecules.[15] The structure and energy of the ion induced dipole H_n^- clusters are investigated with the density functional theory (DFT) method. Recent DFT calculations have predicted unexpected molecular structures for the ion induced dipole H_n^- clusters with the trihydrogen bond.[16,17] The nature of this trihydrogen bond is characterized as $H^-\cdots{}^{\delta+}H\text{-}H^{\delta-}$. Thus, the number of hydrogen atom involved in the hydrogen bond is expanded from one to two, and then to multihydrogen.

Is it possible for the system involving heavy atoms to generate the multihydrogen bond (MHB)? Which kind of environment is suitable for the formation of MHB? How about the nature of the MHB? With the intention to resolve the above questions, this work is carried out with the DFT approach. The following section describes the detailed calculation method. Then, the results and corresponding discussions are represented in the results and discussion part. Main conclusions are collected in the last section.

Calculation Details

The hybrid density functional methods have been prosperously employed in the electronic structure optimizations and the energy determinations. They are uniquely successful in describing large free radicals and intermolecular complexes. The reliability of the B3LYP/6-311++G** basis set level for the MHB system has also been verified by Metta *et al.*[17] Therefore, the whole calculations were all carried out employing the B3LYP approach with the 6-311++G** basis set. Vibrational frequency analysis was performed for each complex at the same level to verify whether the optimized structures correspond to genuine local minima on the global potential energy surface or not. The highest occupied molecular orbital (HOMO) and the lowest unoccupied molecular orbital (LUMO) analyses, as well as the natural bond orbital (NBO) charge population were carried out to explore the nature of the complexes. The orbital interactions between the donor (Lewis type) orbitals and the acceptor (non-Lewis type) orbitals are estimated according to the second-order perturbation theory. For each donor NBO orbital (i) and acceptor NBO orbital (j), the interaction energy E(2) associated with delocalization $i \rightarrow j$ is given by the formula

$$E(2) = \Delta E_{ij} = q_i \cdot F(i,j)^2/(\varepsilon_j - \varepsilon_i) \quad (1)$$

where q_i is the donor orbital occupancy and $F(i,j)$ is the off-diagonal NBO Fock matrix element. ε_i and ε_j are diagonal elements (orbital energies).

The proton chemical shift is determined according to value of TMS. The nuclear magnetic resonance (NMR) spin-spin coupling constant, *J*, is calculated as a sum of the Fermi-contact (FC), spin dipolar (SD), paramagnetic spin-orbital (PSO), and diamagnetic spin-orbit (DSO) contributions.

Results and Discussion

Geometry. The optimized geometry structures of selected MHB systems are all collected in Figure 1. The primary parameters showing the characteristic of these complexes are also represented. For the dimer of hydrogenated HF, F_2^{2-}, the system is in D_{2h} symmetry. There are two excess electrons to enhance the stabilization of the system. The distance between two central hydrogen atoms is 0.828 Å, longer as compared with that of the neutral dihydrogen gas (0.744 Å), the dihydrogen anion (0.772 Å), as well as the dihydrogen with two excess electrons (0.780 Å). The F-H covalent bond distance is 0.937 Å, a little longer than that of the HF monomer, 0.922 Å, indicating the coupling between the central and the terminal hydrogen atoms. The length of central hydrogen and the terminal one is 2.037 Å, which is shorter significantly than the H···e···H distance of anionic $(HF)_2^-$ (2.942 Å).[7] A rhombus structure is generated with four hydrogen atoms. There is only one excess electron is solvated in the hydrogenated HCl dimer system, Cl_2^- which is also in D_{2h} point group. As compared with the distance of two central hydrogen atoms in F_2^{2-}, the distance of the central hydrogen atoms in Cl_2^- system is condensed slightly (0.807 Å). While, the distance between the central hydrogen and the terminal one is extended a little (2.087 Å). The variation of the rhombus structure is slight for these two systems. The length of Cl-H covalent bond is 1.300 Å, longer by 0.013 Å as compared to that of free HCl in the gas phase. There is a four-hydrogen-atom-ring for each of these two systems.

Two imidazole rings populate symmetrically upon the central hydrogen atom in ImH_2^- system. These two rings are almost perpendicular to each other and the system is in C_2 point group. Similarly, the NH bond length is a little longer as compared with that of the free imidazole monomer. The distance between the H_c and the H_t is only 1.379 Å, shorter distinctly than the typical value of nonbonding H···H contacts (2.4 Å). The reported H···e···H distance in anionic imidazole dimer is more than 3.7 Å.[7] One excess electron is solvated in the center of the system. From a geometrical point of view, this is a three-hydrogen-bonded system. For the more complicated system, ImH_4^-, the central hydride is solvated by four imidazole rings. The system is in tetrahedron geometry. The NH covalent bonds are shorter in length by 0.05 Å as compared with those in the ImH_2^- system. While, the distance between the central hydrogen and the terminal

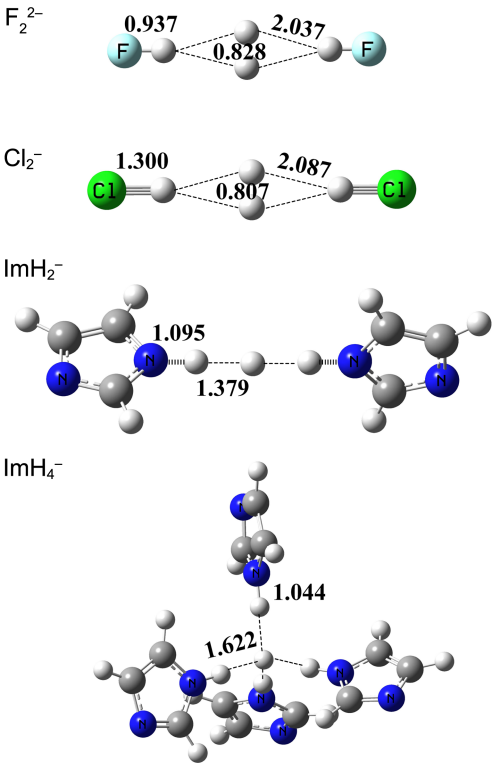

Figure 1. Optimized geometry structures. The bond is represented in Å.

one is 1.622 Å, longer than that in the ImH_2^- system by 0.24 Å. It is clear that this is a five-hydrogen-bonded system.

NBO Charge Analysis. The natural bond orbital (NBO) analysis is carried out for all these systems. The calculated NBO charges of the central hydrogen (Q_c) and the terminal ones (Q_t) are collected in Table 1. In the F_2^{2-} system, the Q_c is −0.909 and the Q_t is −0.592. This indicates that the character of the MHB should be $H^{\delta+}\cdots H_2^{2-}\cdots H^{\delta+}$. Thus, the feature of this system is the four-hydrogen-four-electron (4*H*-4*e*) coupling. The negative charges populate mainly on two central hydrogen atoms, while the terminal hydrogen atom carry distinct positive charge and the F atom is electronegative strongly. The electrostatic interaction between the central hydrogen atoms and the terminal hydrogen/the electronegative F decreases the strength of F-H covalent bond and extends its distance. It is similar for the other systems. The Q_c and Q_t in the Cl_2^- system is −0.381 and 0.305, respectively, demonstrating the feature of this MHB system should be $H^{\delta+}\cdots H_2^-\cdots H^{\delta+}$. The characteristic of this anionic dimer is the four-hydrogen-three-electron (4*H*-3*e*) coupling. The NBO charges on the central hydrogen and the terminal ones in the ImH_2^- system is −0.583 and 0.409, respectively. This MHB system is typical for its $H^{\delta+}\cdots H^-\cdots H^{\delta+}$ structure and the three-hydrogen-two-electron (3*H*-2*e*) coupling. In the complicated ImH_4^- system, the Q_c and Q_t are −0.658 and 0.447, respectively. Although more negative electron populated on the central hydrogen, it is shared by four imidazole rings, instead of two rings in the ImH_2^- system. The characteristic of the ImH_4^- system can be assigned as 5*H*-2*e* coupling. Therefore, the coupling between the central

Table 1. The HOMO and LUMO energies,[a] the NBO charges of the hydrogen,[b] and the NMR parameters[c] of the optimized complexes

	HOMO	LUMO	Q_t	Q_c	σ_t	σ_c	$^1J(H_t\cdots H_c)$	$^1J(H_c\cdots H_c)$	$^2J(H_t\cdots H_t)$
F_2^{2-}	145.3	152.6	0.592	-0.909	-8.4	-74.8	1.0	194.6	0.6
Cl_2^-	51.8	64.8	0.305	-0.381	11.4	-80.5	-0.7	160.5	1.0
ImH_2^-	-37.6	56.6	0.409	-0.583	18.8	7.2	22.4		-9.2
ImH_4^-	-78.3	45.5	0.447	-0.658	15.0	8.0	4.3		0.3

[a]the energies are given in kcal/mol. [b]Q_t and Q_c refer to the NBO charges on the hydrogen atom bonded with the heavy atom and the one populated in the center of the complex, respectively. [c]the unit of σ is ppm and the unit of *J* is in Hz.

and the terminal hydrogen atoms should be weaker, as is reflected by their H···H distances in these two MHB systems. Table 1 illustrates that the H_c is electronegative while the H_t is electropositive for all these four systems.

The NBO analyses also indicate that the couplings between two H_c atoms (68.5 kcal/mol) as well as the interactions between the H_c atoms and the terminal F (68.7 kcal/mol) donate significant contribution to the stability of the F_2^{2-} system. It is the coupling between two H_c atoms (123.3 kcal/mol) stabilizing the Cl_2^- system. While for the ImH_2^- system, the couplings between H_c and two neighbouring N-H groups stabilize the system with the contribution of 183.5 kcal/mol. Four inward N-H groups couple with the H_c atom simultaneously and contribute significantly to the stability by 137.8 kcal/mol.

Electrostatic Potential. The contours of the electrostatic potential of these MHB systems are collected in Figure 2. It is obvious that the negative electrostatic potential (NEP) populates around two H_c atoms located between two HX (X = F, Cl) fragments. This indicates that the excess electrons populate on two H_c atoms, which is in consistent with the results obtained from the NBO analyses. For the ImH_2^- system, distinct NEP can be found around the central hydrogen atom, furthermore, the NEP populate around two terminal imidazole nitrogen atoms. The positive electrostatic potential populates around the C-H bonds of two fragments. Similar phenomena are observed for the ImH_4^- system.

Frontier Molecular Orbitals. Figure 2 also collects the frontier molecular orbitals of these anion systems. The orbitals of F_2^{2-} and Cl_2^- indicate that the multi-hydrogen-bond molecular orbital (MHBMO) populates on four hydrogen atoms, respectively, as demonstrates that the above mentioned 4*H*-4*e* and the 4*H*-3*e* coupling exists for F_2^{2-} and Cl_2^-, respectively. The MHBMO also populates on the hydrogen atoms in the ImH_2^- and ImH_4^- systems. Furthermore, their HOMO orbitals also carry the MHBMO character with the solvated electrons locating between the imidazole ring fragments.

NMR Parameters. The chemical shifts (σ) and the spin-spin coupling constants (^1J(H-H)) are all represented in Table 1. The chemical shift of H_c and H_t in F_2^{2-} is −74.8 and −8.4 ppm, respectively. These values are shifted significantly in Cl_2^- system to −80.5 (low-field) and 11.4 (high-field) ppm, respectively. In the ImH_2^- system, the σ values of H_c and H_t are 7.2 and 18.8, respectively. The σ value of H_c/H_t increases/decreases in ImH_4^- as compared to that in ImH_2^- system. The H_c atoms of F_2^{2-} and Cl_2^{2-} populate in low field, while the central hydrogen atoms of ImH_2^- and ImH_4^- locate in high field, as maybe the result of strong coupling between two central hydrogen atoms. The large $^1J(H_c\cdots H_c)$ value demonstrate the strong interaction between two central hydrogen atoms in F_2^{2-} and Cl_2^- systems. The small value of $^1J(H_t\cdots H_c)$ and $^1J(H_t\cdots H_t)$ illustrate that the weak coupling exists not only between H_c and H_t but also between the terminal hydrogen atoms.

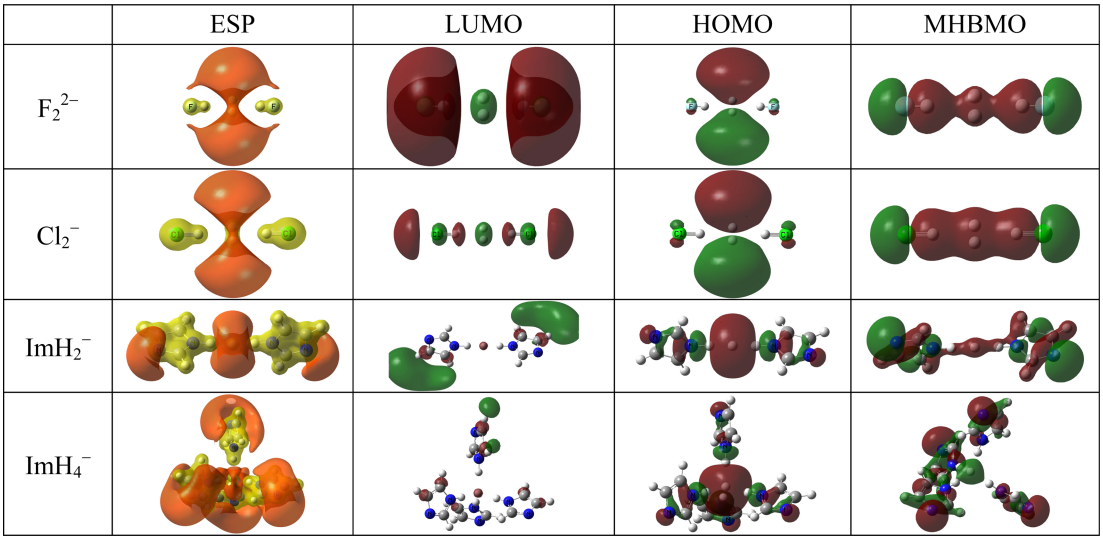

Figure 2. Electrostatic potential, HOMO, LUMO, and the multihydrogen bond molecular orbital (MHBMO) of the optimized geometries.

Concluding Remarks

The multi-hydrogen bonded systems with the solvated electrons are investigated at the B3LYP/6-311++G** basis set level. The linear geometrical characteristic is common for the dimers (F_2^{2-}, Cl_2^-, and ImH_2^-), while for the tetramer system (ImH_4^-), the tetrahedron configuration is generated. The NBO charge analyses demonstrate that the multi-hydrogen-multi-electron (*mH-ne*) coupling exist in these anion systems. The electrostatic potential and the molecular orbital analyses also support the existence of *mH-ne* coupling. Our results also demonstrate that the *mH-ne* coupling is distinct as compared with the H···e···H interactions. The positive chemical shift value of H_c and the negative chemical shift value of H_t indicate that the H_c is electronegative while the H_t is electropositive, respectively. Strong coupling between two central hydrogen atoms is demonstrated by large chemical shifts and big spin-spin coupling constants.

Acknowledgments. The publication cost of this paper was supported by the Korean Chemical Society.

References

1. Bakhmutov, V. I. *Dihydrogen Bonds: Principles, Experiments, and Applications*; Wiley-Interscience: Hoboken, NJ, 2008.
2. Grabowski, S. J.; Sokalski, W. A.; Leszczynski, J. *J. Phys. Chem. A* **2004**, *108*, 5823.
3. Alkorta, I.; Rozas, I.; Elguero, J. *Chem. Soc. Rev.* **1998**, *27*, 163.
4. Crabtree, R. H. *Science* **1998**, *282*, 2000.
5. Crabtree, R. H.; Siegbahn, P. E. M.; Eisenstein, O.; Rheingold, A. L.; Koetzle, T. F. *Acc. Chem. Res.* **1996**, *29*, 348.
6. Hao, X. Y.; Li, Z. R.; Wu, D.; Li, Z. S.; Sun, C. C. *J. Chem. Phys.* **2003**, *118*, 10939.
7. Yan, S. H.; Bu, Y. X.; Cukier, R. I. *J. Chem. Phys.* **2006**, *124*, 124314.
8. Kim, K. S.; Lee, S.; Kim, J.; Lee, J. Y. *J. Am. Chem. Soc.* **1997**, *119*, 9329.
9. Zhang, L.; Yan, S. H.; Cukier, R. I.; Bu, Y. X. *J. Phys. Chem. B* **2008**, *112*, 3767.
10. Kim, K. S.; Park, I.; Lee, S.; Cho, K.; Lee, J. Y.; Kim, J.; Joannopoulos, J. D. *Phys. Rev. Lett.* **1996**, *76*, 956.
11. Hao, X. Y.; Li, Z. R.; Wu, D.; Wang, Y.; Li, Z. S.; Sun, C. C. *J. Chem. Phys.* **2003**, *118*, 83.
12. Yan, S. H.; Lee, J. Y. *J. Phys. Chem. C* **2009**, *113*, 1104.
13. McCall, B. J.; Geballe, T. R.; Hinkle, K. H.; Oka, T. *Science* **1998**, *279*, 1910.
14. McCall, B. J.; Oka, T. *Science* **2000**, *287*, 1941.
15. Chávez-Calvillo, R.; Hernández-Trujillo, J. *J. Phys. Chem. A* **2011**, *115*, 13036.
16. Huang, L.; Matta, C. F.; Massa, L. *J. Phys. Chem. A* **2011**, *115*, 12445.
17. Matta, C. F.; Huang, L. L.; Massa, L. *J. Phys. Chem. A* **2011**, *115*, 12451.